On thermodynamic self-consistency of generic axiomatic-nonextensive statistics

Abdel Nasser Tawfik[1,2;1)] Hayam Yassin[3] Eman R. Abo Elyazeed[3]

[1]Egyptian Center for Theoretical Physics (ECTP), Modern University for Technology and Information (MTI), 11571 Cairo, Egypt
[2]World Laboratory for Cosmology and Particle Physics (WLCAPP), 11571 Cairo, Egypt
[3]Physics Department, Faculty of Women for Arts, Science and Education, Ain Shams University, 11577 Cairo, Egypt

Abstract: Generic axiomatic-nonextensive statistics introduces two asymptotic properties, to each of which a scaling function is assigned. The first and second scaling properties are characterized by the exponents c and d, respectively. In the thermodynamic limit, a grand-canonical ensemble can be formulated. The thermodynamic properties of a relativistic ideal gas of hadron resonances are studied, analytically. It is found that this generic statistics satisfies the requirements of the equilibrium thermodynamics. Essential aspects of the thermodynamic self-consistency are clarified. Analytical expressions are proposed for the statistical fits of various transverse momentum distributions measured in most-central collisions at different collision energies and colliding systems. Estimations for the freezeout temperature ($T_{\mathtt{ch}}$) and the baryon chemical potential ($\mu_{\mathtt{b}}$) and the exponents c and d are determined. The earlier are found compatible with the parameters deduced from Boltzmann-Gibbs (BG) statistics (extensive), while the latter refer to generic nonextensivities. The resulting equivalence class (c, d) is associated with stretched exponentials, where Lambert function reaches its asymptotic stability. In some measurements, the resulting nonextensive entropy is linearly composed on extensive entropies. Apart from power-scaling, the particle ratios and yields are excellent quantities to highlighting whether the particle production takes place (non)extensively. Various particle ratios and yields measured by the STAR experiment in central collisions at 200, 62.4 and 7.7 GeV are fitted with this novel approach. We found that both c and $d < 1$, i.e. referring to neither BG- nor Tsallis-type statistics, but to (c, d)-entropy, where Lambert functions exponentially rise. The freezeout temperature and baryon chemical potential are found comparable with the ones deduced from BG statistics (extensive). We conclude that the particle production at STAR energies is likely a nonextensive process but not necessarily BG or Tsallis type.

Keywords: Nonextensive thermodynamical consistency, Boltzmann and Fermi-Dirac statistics

PACS: 05.70.Ln, 05.70.Fh,05.70.Ce **DOI:** 10.1088/1674-1137/41/5/053107

1 Introduction

In theories of extensive (such as Boltzmann-Gibbs) and nonextensive (such as Tsallis) statistics, thermodynamic consistency gives a phenomenological description for various phenomena in high-energy experiments [1, 2]. The earlier was used by Hagedorn [3] in the 1960s to prove that fireballs or heavy resonances lead to a bootstrap approach, i.e. further fireballs, which - in turn - consist of smaller fireballs and so on. The implementation of the nonextensive Tsallis statistics was introduced in Refs. [5–7]. Assuming that the distribution function can vary, due to possible symmetrical change, Tawfik applied nonextensive concepts to high-energy particle production [4]. Recently, various papers were quite successful in explaining various aspects of high-energy particle production using thermodynamically consistent nonextensive statistics of Tsallis type [8–14]. These are based on the conjecture that replacing the Boltzmann factor by the q-exponential function of Tsallis statistics, with $q > 1$, leads to a good agreement with the experimental measurements at high energies. Recently, Tawfik explained that this method seems to fail to assure a full incorporation of nonextensivity because fluctuations, correlations, interactions among the produced particles besides the possible modification in the phase space of such an interacting system are not properly taken into account [15]. Again, the Tsallis distribution was widely applied to describe the hadron production [8–14]. At high transverse momentum spectra (p_T), some authors did not obtain a power-law, while at low p_T, they obtained an approximate exponential distribution.

In light of such a wide discrepancy, and especially to find a unified statistical description for high-energy collisions, we introduce generic axiomatic-nonextensive

Received 21 December 2016, Revised 23 December 2016

1) E-mail: a.tawfik@eng.mti.edu.eg

statistics, in which the phase space determines the degree of (non)extensivity. The latter is not necessarily limited to extensive and/or intensive thermodynamic quantities, such as temperature and baryon chemical potential.

Regarding the success of Tsallis statistics in describing transverse momentum spectra, especially at high p_T, we first recall that Bialas claimed that such a good fit would be incomplete [16]. First, it is believed to ignore the contradiction between the applicability of such a statistical thermal approach at high energy and perturbative QCD. The crucial question which should be answered is how the statistical thermal approach, which describes lattice thermodynamics (non-perturbative) [1] well, can be assumed to do such an excellent job at ultra-relativistic energies. Second, such a statistical fit seems to disbelieve the role of statistical cluster decay, which can be scaled as power laws very similar to that from Tsallis statistics. This simply means that the decay of statistical clusters is conjectured to be capable of explaining the excellent reproduction of the measured transverse momenta rather than the Tsallis-type nonextensivity [15].

Also, Bialas [16] presented within the statistical cluster-decay model a numerical analysis for the hadronization processes. It was found that the resulting transverse-momentum distribution can be a Tsallis-like one. Only in a very special case, where the fluctuations of the Lorentz factor and the temperature are given by Beta and Gamma distributions, respectively, can the well-known Tsallis distribution be obtained. The origin of these fluctuations was introduced in Ref. [17]. Bialas explained the produced hadronic cluster decays purely thermally, i.e. following Boltzmann-Gibbs (BG) statistics [16]. Furthermore, it is also supposed that the produced hadronic clusters move with a fluctuating Lorentz factor in the transverse direction, i.e. a power law. Thus, the production and the decay of such clusters would be be regarded as examples of superstatistics. The latter can be understood as a kind of a superposition of two different types of statistics corresponding to nonequilibrium systems [18, 19]. In other words, it was concluded [17] that even superstatistics should be based on more general distributions than the Gamma type before being applied to multiparticle productions in high energy collisions. For the sake of completeness, we recall that the various power-law distributions have been already implemented in pp-collisions [20–24].

The crucial questions that remains unanswered are what the origin and degree of nonextensivity are, and how the degree of nonextensivity can be determined in a strongly correlated system, such as relativistic heavy-ion collisions. In the present work, we analyse the thermodynamic self-consistency of the generic axiomatic-nonextensive approach, which was introduced in [25, 26] and formulated for further implications in high-energy physics in Refs. [15, 27].

In thermal equilibrium, statistical mechanics is a thermodynamically self-consistent theory. It fulfils the requirements of equilibrium thermodynamics, because a thermodynamic potential - in its thermodynamic limit - can be expressed as a first-order homogeneous function of extensive variables [28]. The entropy is a fundamental check for thermodynamic self-consistency. For a nonextensive quantum gas, the entropy should be fully constructed from boson and fermion contributions: $S_q=S_q^{\rm FD}+S_q^{\rm BE}$, where $S_q^{\rm FD}$ and $S_q^{\rm BE}$ are Fermi-Dirac and Bose-Einstein nonextensive entropy, respectively [29]. In microcanonical [30], canonical [31], and grand canonical [32] ensembles, the thermodynamic self-consistency of Tsallis statistics has been proved. If its entropic variable is extensive, it has been demonstrated that the homogeneity of the thermodynamic potential leads to the zeroth law of thermodynamics, i.e. the additivity principle and Euler theorem. Also, the first and second laws of thermodynamics should be fulfilled. An additional ingredient of special importance in that particle production, namely the fireball self-consistency principle, should be guaranteed as well.

This paper is organized as follows. Generic axiomatic-nonextensive statistics is reviewed in Section 2. Thermodynamic self-consistency is discussed in Section 3. This is divided into nonextensive Boltzmann-Gibbs statistics (Section 3.1) and generic axiomatic-nonextensive quantum statistics (Section 3.2). Sections 4 and 4.2 are devoted to the fitting of the transverse momentum distributions and particle ratios with different beam energies and different system sizes, respectively. Section 5 gives the final conclusions.

2 Generic axiomatic-nonextensive statistics

Based on Hanel-Thurner entropy [25–27], which is fully expressed in Ref. [15],

$$S_{c,d}[p]=\sum_{i=1}^{\Omega}\mathcal{A}\Gamma(d+1,1-c\log p_i)-\mathcal{B}p_i, \qquad (1)$$

where p_i is the probability of the i-th state and $\Gamma(a,b)=\int_b^{\infty}\mathrm{d}t\, t^{a-1}\exp(-t)$ is an incomplete gamma-function with $\mathcal{A}$ and $\mathcal{B}$ being arbitrary parameters, the generic axiomatic-nonextensive partition function for statistical processes in high-energy physics was suggested [27]. For a classical gas,

$$\ln Z_{\rm cl}(T,\mu)=V\sum_i^{N_{\rm M|B}} g_i\int_0^{\infty}\frac{\mathrm{d}^3\boldsymbol{p}}{(2\pi)^3}\,\varepsilon_{c,d,r}(x_i), \qquad (2)$$

where V is the fireball volume and $x_i = \beta[\mu_i - E_i(\boldsymbol{p})]$ with $E_i(p) = (\boldsymbol{p}^2+m_i^2)^{1/2}$ is the dispersion relation of the i-th state (particle). Straightforwardly, the quantum gas partition function reads

$$\ln Z_{\mathtt{FB}}(T) = \pm V \sum_{i}^{N_{\mathtt{M|B}}} g_i \int_0^{\infty} \frac{\mathrm{d}^3\boldsymbol{p}}{(2\pi)^3} \ln[1 \pm \varepsilon_{c,d,r}(x_i)], \quad (3)$$

where $\pm$ represent fermions (subscript F) and bosons (subscript B), respectively. The distribution function $\varepsilon_{c,d,r}(x_i)$ is given as [25, 26]

$$\varepsilon_{c,d,r}(x) = \exp\left[\frac{-d}{1-c}\left(W_k\left[B\left(1-\frac{x}{r}\right)^{\frac{1}{d}}\right] - W_k[B]\right)\right], \quad (4)$$

where W_k is the Lambert W-function which has real solutions at $k=0$ with $d \geqslant 0$ and at $k=1$ with $d<0$,

$$B = \frac{(1-c)r}{1-(1-c)r} \exp\left[\frac{(1-c)r}{1-(1-c)r}\right], \quad (5)$$

with $r = [1-c+cd]^{-1}$ and c,d being two constants to be elaborated shortly. Equation (4) is valid for both classical and quantum gases.

The equivalent classes (c,d) stand for two exponents giving estimations for two scaling functions with two asymptotic properties [25, 26]. Statistical systems in their large size limit violating the fourth Shannon-Khinchin axiom are characterized by a unique pair of scaling exponents (c,d). Such systems have two asymptotic properties of their associated generalized entropies. Both properties are associated with one scaling function each. Each scaling function is characterized by one exponent; c for the first and d for the second property. These exponents define equivalence relations of entropic forms, i.e. two entropic forms are equivalent if their exponents are the same.

The various thermodynamic observables such as pressure (p), number ($n = N/V$), energy ($\epsilon = E/V$) and entropy density ($s = S/V$) [33] can be derived from Eq. (2) or Eq. (3).

$$p = T\frac{\partial \ln Z}{\partial V}, \qquad n = \frac{\partial p}{\partial \mu},$$

$$\epsilon = \frac{T^2}{V}\frac{\partial \ln Z}{\partial T} + \frac{\mu T}{V}\frac{\partial \ln Z}{\partial \mu}, \qquad s = \frac{\partial p}{\partial T}. \quad (6)$$

3 Thermodynamic self-consistency

Here, we examine the thermodynamic self-consistency of generic axiomatic-nonextensive statistics in Boltzmann-Gibbs and quantum gases. The procedure goes as follows. We start with the first and second laws of thermodynamics which control the system of interest. Then, we determine the thermodynamic properties of that system and confirm that both laws of thermodynamics are verified.

The first law of thermodynamics describes the change in energy ($\mathrm{d}E$) in terms of a change in volume ($\mathrm{d}V$) and entropy ($\mathrm{d}S$):

$$\mathrm{d}E(V,S) = -P\,\mathrm{d}V + T\,\mathrm{d}S, \quad (7)$$

where T and P are temperature and pressure coefficients, respectively. In the variation of the free energy, $F(V,T) = E - T\,S$, the dependence on the entropy as given in Eq. (7) is to be replaced by a temperature-dependence

$$\mathrm{d}F(V,T) = \mathrm{d}E - T\,\mathrm{d}S - S\,\mathrm{d}T \equiv -P\,\mathrm{d}V - S\,\mathrm{d}T. \quad (8)$$

If the system of interest contains a conserved number (N), it is necessary to introduce a chemical potential (μ). Equations (7) and (8) should be extended as

$$\mathrm{d}E(V,S,N) = -P\,\mathrm{d}V + T\,\mathrm{d}S + \mu\,\mathrm{d}N, \quad (9)$$

$$\mathrm{d}F(V,T,\mu) = -P\,\mathrm{d}V - S\,\mathrm{d}T - N\,\mathrm{d}\mu. \quad (10)$$

The pressure is derived as

$$p = -\left.\frac{\partial F}{\partial V}\right|_{T,\mu}. \quad (11)$$

From Eqs. (2), (3) and (11), thermodynamics relations can be deduced [33]. Their justification proves the thermodynamic self-consistency,

$$n = \left.\frac{\partial p}{\partial \mu}\right|_T, \quad T = \left.\frac{\partial \epsilon}{\partial s}\right|_n, \quad s = \left.\frac{\partial p}{\partial T}\right|_\mu, \quad \mu = \left.\frac{\partial \epsilon}{\partial n}\right|_s. \quad (12)$$

To verify the second law of thermodynamics one has to prove that $\partial s \geqslant 0$.

In the section that follows, all these thermodynamic quantities shall be derived from the generic axiomatic-nonextensive statistics for Boltzmann-Gibbs, Bose-Einstein and Fermi-Dirac statistical ensembles [32].

3.1 Nonextensive Boltzmann-Gibbs statistics

As discussed in Ref. [34], the universality class (c,d) is conjectured not only to characterize the entropy of the system of interest entirely, but also to specify the distribution functions of that system in the thermodynamic limit. Thus, it is likely able to determine the (non)extensivity of the system. For instance, if $(c,d) = (1,1)$, the system can be well described by BG statistics, while if $(c,d) = (q,0)$, the system has a Tsallis-type nonextensivity. Furthermore, if $(c,d) = (1,d)$, stretched exponentials characterize that system. To our knowledge, further details about the physical meaning of (c,d) are being worked out by many colleagues and should be published in the near future. The last case, for instance, requires that $d>0$ and $c\rightarrow 1$ so that $\lim_{c\rightarrow 1}\varepsilon_{c,d,r}(x)=\exp(-\mathrm{d}r[1-x/r]^{1/d}-1)$. In light of this, for a single particle, the Boltzmann distribution in a nonextensive system, Eq. (2), can be expressed as

$$f(x)=\frac{1}{\varepsilon_{c,d,r}(x)}, \tag{13}$$

from which various thermodynamic quantities can deduced

$$p=\frac{gT}{2\pi^2}\int_0^\infty \boldsymbol{p}^2\ln\left[\varepsilon_{c,d,r}(x)\right]\mathrm{d}\boldsymbol{p}, \tag{14}$$

$$n=\frac{g}{2\pi^2}\int_0^\infty \frac{\boldsymbol{p}^2\, W_0\left[B\left(1-\frac{x}{r}\right)^{\frac{1}{d}}\right]}{(1-c)\left[r-x\right]\left(1+W_0\left[B\left(1-\frac{x}{r}\right)^{\frac{1}{d}}\right]\right)}\mathrm{d}\boldsymbol{p}, \tag{15}$$

$$\epsilon=\frac{-g}{2\pi^2}\int_0^\infty \frac{\boldsymbol{p}^2(x\,T)\, W_0\left[B\left(1-\frac{x}{r}\right)^{\frac{1}{d}}\right]}{(1-c)\left[r-x\right]\left(1+W_0\left[B\left(1-\frac{x}{r}\right)^{\frac{1}{d}}\right]\right)}\mathrm{d}\boldsymbol{p} + \frac{g\,\mu}{2\pi^2}\int_0^\infty \frac{\boldsymbol{p}^2\, W_0\left[B\left(1-\frac{x}{r}\right)^{\frac{1}{d}}\right]}{(1-c)\left[r-x\right]\left(1+W_0\left[B\left(1-\frac{x}{r}\right)^{\frac{1}{d}}\right]\right)}\mathrm{d}\boldsymbol{p}, \tag{16}$$

$$s=\frac{g}{2\pi^2}\int_0^\infty \boldsymbol{p}^2\ln\left[\varepsilon_{c,d,r}(x)\right]\mathrm{d}\boldsymbol{p} - \frac{g}{2\pi^2 T}\int_0^\infty \frac{\boldsymbol{p}^2\,(x\,T)\, W_0\left[B\left(1-\frac{x}{r}\right)^{\frac{1}{d}}\right]}{(1-c)\left[r-x\right]\left(1+W_0\left[B\left(1-\frac{x}{r}\right)^{\frac{1}{d}}\right]\right)}\mathrm{d}\boldsymbol{p}. \tag{17}$$

In an ideal gas approach, such as the hadron resonance gas (HRG) model, the thermodynamic quantities get contributions from each hadron resonance. Thus, a summation over the different hadron resonances of which the statistical ensemble consists should be added in front of the right-hand side.

To check and satisfy the thermodynamic self-consistency, let us rewrite Eq. (17) as

$$s=\frac{p}{T}+\frac{\epsilon}{T}-\frac{\mu\, n}{T}, \tag{18}$$

and take its derivative with respect to ϵ. We then get

$$\left.\frac{\partial s}{\partial \epsilon}\right|_n=\frac{1}{T}. \tag{19}$$

Furthermore, we derive from Eq. (2) [33],

$$p=-\epsilon+T\,s+\mu\, n. \tag{20}$$

At constant T, the derivative of pressure with respect to μ reads

$$\left.\frac{\partial p}{\partial \mu}\right|_T=-\frac{\partial \epsilon}{\partial \mu}+T\frac{\partial s}{\partial \mu}+n+\mu\frac{\partial n}{\partial \mu}. \tag{21}$$

The differentiations of Eqs. (15), (16), and (17) with respect to μ lead to

$$\frac{\partial n}{\partial \mu}=\frac{g}{2\pi^2 T}\int_0^\infty \frac{\boldsymbol{p}^2\, W_0\left[B\left(1-\frac{x}{r}\right)^{\frac{1}{d}}\right]^2}{(d-d\,c)r^2\,(1-x/r)^2\left(1+W_0\left[B\left(1-\frac{x}{r}\right)^{\frac{1}{d}}\right]\right)^3}\mathrm{d}\boldsymbol{p} - \frac{g}{2\pi^2 T}\int_0^\infty \frac{\boldsymbol{p}^2\, W_0\left[B\left(1-\frac{x}{r}\right)^{\frac{1}{d}}\right]}{(d-d\,c)r^2\,(1-x/r)^2\left(1+W_0\left[B\left(1-\frac{x}{r}\right)^{\frac{1}{d}}\right]\right)^2}\mathrm{d}\boldsymbol{p} + \frac{g}{2\pi^2 T}\int_0^\infty \frac{\boldsymbol{p}^2\, W_0\left[B\left(1-\frac{x}{r}\right)^{\frac{1}{d}}\right]}{(1-c)r^2\,(1-x/r)^2\left(1+W_0\left[B\left(1-\frac{x}{r}\right)^{\frac{1}{d}}\right]\right)}\mathrm{d}\boldsymbol{p}, \tag{22}$$

$$\frac{\partial \epsilon}{\partial \mu}=\frac{g\,\mu}{2\pi^2 T}\int_0^\infty \frac{\boldsymbol{p}^2\left(W_0\left[B\left(1-\frac{x}{r}\right)^{\frac{1}{d}}\right]\right)^2}{(d-d\,c)r^2\,(1-x/r)^2\left(1+W_0\left[B\left(1-\frac{x}{r}\right)^{\frac{1}{d}}\right]\right)^3}\mathrm{d}\boldsymbol{p}$$

$$-\frac{g\,\mu}{2\pi^2 T}\int_0^\infty \frac{\boldsymbol{p}^2\,W_0\left[B\left(1-\frac{x}{r}\right)^{\frac{1}{d}}\right]}{(d-d\,c)r^2\,(1-x/r)^2\left(1+W_0\left[B\left(1-\frac{x}{r}\right)^{\frac{1}{d}}\right]\right)^2}\mathrm{d}\boldsymbol{p}$$

$$+\frac{g\,\mu}{2\pi^2 T}\int_0^\infty \frac{\boldsymbol{p}^2\,W_0\left[B\left(1-\frac{x}{r}\right)^{\frac{1}{d}}\right]}{(1-c)r^2\,(1-x/r)^2\left(1+W_0\left[B\left(1-\frac{x}{r}\right)^{\frac{1}{d}}\right]\right)}\mathrm{d}\boldsymbol{p}$$

$$-\frac{g}{2\pi^2 T}\int_0^\infty \frac{\boldsymbol{p}^2\,(x\,T)\,W_0\left[B\left(1-\frac{x}{r}\right)^{\frac{1}{d}}\right]^2}{(d-d\,c)r^2\,(1-x/r)^2\left(1+W_0\left[B\left(1-\frac{x}{r}\right)^{\frac{1}{d}}\right]\right)^3}\mathrm{d}\boldsymbol{p}$$

$$+\frac{g}{2\pi^2 T}\int_0^\infty \frac{\boldsymbol{p}^2\,(x\,T)\,W_0\left[B\left(1-\frac{x}{r}\right)^{\frac{1}{d}}\right]}{(d-d\,c)r^2\,(1-x/r)^2\left(1+W_0\left[B\left(1-\frac{x}{r}\right)^{\frac{1}{d}}\right]\right)^2}\mathrm{d}\boldsymbol{p}$$

$$-\frac{g}{2\pi^2 T}\int_0^\infty \frac{\boldsymbol{p}^2\,(x\,T)\,W_0\left[B\left(1-\frac{x}{r}\right)^{\frac{1}{d}}\right]}{(1-c)r^2\,(1-x/r)^2\left(1+W_0\left[B\left(1-\frac{x}{r}\right)^{\frac{1}{d}}\right]\right)}\mathrm{d}\boldsymbol{p}, \tag{23}$$

$$\frac{\partial s}{\partial \mu}=\frac{-g}{2\pi^2 T^2}\int_0^\infty \frac{\boldsymbol{p}^2\,(x\,T)\,W_0\left[B\left(1-\frac{x}{r}\right)^{\frac{1}{d}}\right]^2}{(d-d\,c)r^2\,(1-x/r)^2\left(1+W_0\left[B\left(1-\frac{x}{r}\right)^{\frac{1}{d}}\right]\right)^3}\mathrm{d}\boldsymbol{p}$$

$$+\frac{g}{2\pi^2 T^2}\int_0^\infty \frac{\boldsymbol{p}^2\,(x\,T)\,W_0\left[B\left(1-\frac{x}{r}\right)^{\frac{1}{d}}\right]}{(d-d\,c)r^2\,(1-x/r)^2\left(1+W_0\left[B\left(1-\frac{x}{r}\right)^{\frac{1}{d}}\right]\right)^2}\mathrm{d}\boldsymbol{p}$$

$$-\frac{g}{2\pi^2 T^2}\int_0^\infty \frac{\boldsymbol{p}^2\,(x\,T)\,W_0\left[B\left(1-\frac{x}{r}\right)^{\frac{1}{d}}\right]}{(1-c)r^2\,(1-x/r)^2\left(1+W_0\left[B\left(1-\frac{x}{r}\right)^{\frac{1}{d}}\right]\right)}\mathrm{d}\boldsymbol{p}. \tag{24}$$

Then, the substitution from Eqs. (15), (22), (23) and (24) into Eq. (21) gives

$$\left.\frac{\partial p}{\partial \mu}\right|_T = n. \tag{25}$$

Also, from Eq. (18) we can express the energy density as

$$\epsilon = T\,s - p + \mu\,n, \tag{26}$$

Its differentiation with respect to n is

$$\left.\frac{\partial \epsilon}{\partial n}\right|_s = -\frac{\partial p}{\partial n} + \mu + n\frac{\partial \mu}{\partial n} = -\frac{\partial p}{\partial \mu}\frac{\partial \mu}{\partial n} + \mu + n\frac{\partial \mu}{\partial n}. \tag{27}$$

By substituting from Eq. (25) into this previous equation, we get

$$\left.\frac{\partial \epsilon}{\partial n}\right|_s = \mu, \tag{28}$$

which is a proof of thermodynamic self-consistency.

To prove the fourth equation in Eq. (12), let us differentiate Eq. (20) with respect to temperature at constant μ

$$\left.\frac{\partial p}{\partial T}\right|_\mu = s + T\frac{\partial s}{\partial T} - \frac{\partial \epsilon}{\partial T} + \mu\frac{\partial n}{\partial T}, \tag{29}$$

The differentiations of Eqs. (15), (16) and (17) with respect to T read

$$\begin{aligned}\frac{\partial n}{\partial T}=&\frac{-g}{2\pi^2T^2}\int_0^\infty\frac{\boldsymbol{p}^2\,(x\,T)\,W_0\left[B\left(1-\frac{x}{r}\right)^{\frac{1}{d}}\right]^2}{(d-d\,c)r^2\,(1-x/r)^2\left(1+W_0\left[B\left(1-\frac{x}{r}\right)^{\frac{1}{d}}\right]\right)^3}\mathrm{d}\boldsymbol{p}\\&+\frac{g}{2\pi^2T^2}\int_0^\infty\frac{\boldsymbol{p}^2\,(x\,T)\,W_0\left[B\left(1-\frac{x}{r}\right)^{\frac{1}{d}}\right]}{(d-d\,c)r^2\,(1-x/r)^2\left(1+W_0\left[B\left(1-\frac{x}{r}\right)^{\frac{1}{d}}\right]\right)^2}\mathrm{d}\boldsymbol{p}\\&-\frac{g}{2\pi^2T^2}\int_0^\infty\frac{\boldsymbol{p}^2\,(x\,T)\,W_0\left[B\left(1-\frac{x}{r}\right)^{\frac{1}{d}}\right]}{(1-c)r^2\,(1-x/r)^2\left(1+W_0\left[B\left(1-\frac{x}{r}\right)^{\frac{1}{d}}\right]\right)}\mathrm{d}\boldsymbol{p},\end{aligned}\tag{30}$$

$$\begin{aligned}\frac{\partial \epsilon}{\partial T}=&\frac{g}{2\pi^2T^2}\int_0^\infty\frac{\boldsymbol{p}^2\,(x\,T)^2\,W_0\left[B\left(1-\frac{x}{r}\right)^{\frac{1}{d}}\right]^2}{(d-d\,c)r^2\,(1-x/r)^2\left(1+W_0\left[B\left(1-\frac{x}{r}\right)^{\frac{1}{d}}\right]\right)^3}\mathrm{d}\boldsymbol{p}\\&-\frac{g}{2\pi^2T^2}\int_0^\infty\frac{\boldsymbol{p}^2\,(x\,T)^2\,W_0\left[B\left(1-\frac{x}{r}\right)^{\frac{1}{d}}\right]}{(d-d\,c)r^2\,(1-x/r)^2\left(1+W_0\left[B\left(1-\frac{x}{r}\right)^{\frac{1}{d}}\right]\right)^2}\mathrm{d}\boldsymbol{p}\\&+\frac{g}{2\pi^2T^2}\int_0^\infty\frac{\boldsymbol{p}^2\,(x\,T)^2\,W_0\left[B\left(1-\frac{x}{r}\right)^{\frac{1}{d}}\right]}{(1-c)r^2\,(1-x/r)^2\left(1+W_0\left[B\left(1-\frac{x}{r}\right)^{\frac{1}{d}}\right]\right)}\mathrm{d}\boldsymbol{p}\\&-\frac{g\,\mu}{2\pi^2T^2}\int_0^\infty\frac{\boldsymbol{p}^2\,(x\,T)\,\left(W_0\left[B\left(1-\frac{x}{r}\right)^{\frac{1}{d}}\right]\right)^2}{(d-d\,c)r^2\,(1-x/r)^2\left(1+W_0\left[B\left(1-\frac{x}{r}\right)^{\frac{1}{d}}\right]\right)^3}\mathrm{d}\boldsymbol{p}\\&+\frac{g\,\mu}{2\pi^2T^2}\int_0^\infty\frac{\boldsymbol{p}^2\,(x\,T)\,W_0\left[B\left(1-\frac{x}{r}\right)^{\frac{1}{d}}\right]}{(d-d\,c)r^2\,(1-x/r)^2\left(1+W_0\left[B\left(1-\frac{x}{r}\right)^{\frac{1}{d}}\right]\right)^2}\mathrm{d}\boldsymbol{p}\\&-\frac{g\,\mu}{2\pi^2T^2}\int_0^\infty\frac{\boldsymbol{p}^2\,(x\,T)\,W_0\left[B\left(1-\frac{x}{r}\right)^{\frac{1}{d}}\right]}{(1-c)r^2\,(1-x/r)^2\left(1+W_0\left[B\left(1-\frac{x}{r}\right)^{\frac{1}{d}}\right]\right)}\mathrm{d}\boldsymbol{p},\end{aligned}\tag{31}$$

$$\begin{aligned}\frac{\partial s}{\partial T}=&\frac{g}{2\pi^2T^3}\int_0^\infty\frac{\boldsymbol{p}^2\,(x\,T)^2\,W_0\left[B\left(1-\frac{x}{r}\right)^{\frac{1}{d}}\right]^2}{(d-d\,c)r^2\,(1-x/r)^2\left(1+W_0\left[B\left(1-\frac{x}{r}\right)^{\frac{1}{d}}\right]\right)^3}\mathrm{d}\boldsymbol{p}\\&-\frac{g}{2\pi^2T^3}\int_0^\infty\frac{\boldsymbol{p}^2\,(x\,T)^2\,W_0\left[B\left(1-\frac{x}{r}\right)^{\frac{1}{d}}\right]}{(d-d\,c)r^2\,(1-x/r)^2\left(1+W_0\left[B\left(1-\frac{x}{r}\right)^{\frac{1}{d}}\right]\right)^2}\mathrm{d}\boldsymbol{p}\end{aligned}$$

$$+\frac{g}{2\pi^2 T^3}\int_0^\infty \frac{\boldsymbol{p}^2\,(x\,T)^2\,W_0\left[B\left(1-\frac{x}{r}\right)^{\frac{1}{d}}\right]}{(1-c)r^2\,(1-x/r)^2\left(1+W_0\left[B\left(1-\frac{x}{r}\right)^{\frac{1}{d}}\right]\right)}\mathrm{d}\boldsymbol{p}. \tag{32}$$

Then, the substitution from Eqs. (17), (30), (31) and (32) into Eq. (29) leads to

$$\left.\frac{\partial p}{\partial T}\right|_{\mu}=s. \tag{33}$$

It is apparent that the given definitions of temperature, number density, chemical potential and entropy density are thermodynamically consistent.

The first law of thermodynamics describes the consequences of heat transfer, Eq. (18), while the second law sets constraints on it, i.e. $\delta s\geqslant 0$,

$$\partial s\simeq\frac{1}{T}\left[\partial\epsilon-\mu\partial n\right], \tag{34}$$

where $\partial\mu/\partial T$ is conjectured to vanish. Therefore, the second law of thermodynamics is fulfilled, if

$$\partial\epsilon\geqslant\mu\partial n. \tag{35}$$

This inequality is fulfilled, when comparing Eq. (30) with Eq. (31). Two cases can be classified. Firstly, $\partial\epsilon>\mu\partial n$ is obvious, at arbitrary μ. Secondly, $\partial\epsilon=\mu\partial n$ is also obtained, at $c=1$ or $\mu=\epsilon$ or $\mu=\epsilon+Tr$.

3.2 Generic axiomatic-nonextensive quantum statistics

For quantum statistics, the distribution function reads

$$f(x)=\frac{1}{1\pm\varepsilon_{c,d,r}(x)}, \tag{36}$$

Accordingly, the various thermodynamic quantities can be deduced

$$p=\frac{gT}{2\pi^2}\int_0^\infty \boldsymbol{p}^2\ln\left[1\pm\varepsilon_{c,d,r}(x)\right]\mathrm{d}\boldsymbol{p}, \tag{37}$$

$$n=\frac{\pm g}{2\pi^2}\int_0^\infty \frac{\boldsymbol{p}^2\,\varepsilon_{c,d,r}(x)\,W_0\left[B\left(1-\frac{x}{r}\right)^{\frac{1}{d}}\right]}{(1-c)\left[1\pm\varepsilon_{c,d,r}(x)\right](r-x)\left(1+W_0\left[B\left(1-\frac{x}{r}\right)^{\frac{1}{d}}\right]\right)}\mathrm{d}\boldsymbol{p}, \tag{38}$$

$$\epsilon=\frac{\mp g}{2\pi^2}\int_0^\infty \frac{\boldsymbol{p}^2\varepsilon_{c,d,r}(x)\,(x\,T)\,W_0\left[B\left(1-\frac{x}{r}\right)^{\frac{1}{d}}\right]}{(1-c)\left[1\pm\varepsilon_{c,d,r}(x)\right](r-x)\left(1+W_0\left[B\left(1-\frac{x}{r}\right)^{\frac{1}{d}}\right]\right)}\mathrm{d}\boldsymbol{p}$$

$$\pm\frac{g\mu}{2\pi^2}\int_0^\infty \frac{\boldsymbol{p}^2\varepsilon_{c,d,r}(x)\,W_0\left[B\left(1-\frac{x}{r}\right)^{\frac{1}{d}}\right]}{(1-c)\left[1\pm\varepsilon_{c,d,r}(x)\right](r-x)\left(1+W_0\left[B\left(1-\frac{x}{r}\right)^{\frac{1}{d}}\right]\right)}\mathrm{d}\boldsymbol{p}, \tag{39}$$

$$s=\frac{g}{2\pi^2}\int_0^\infty \boldsymbol{p}^2\ln\left[1\pm\varepsilon_{c,d,r}(x)\right]\mathrm{d}\boldsymbol{p}\pm\frac{g}{2\pi^2 T}\int_0^\infty \frac{\boldsymbol{p}^2\,\varepsilon_{c,d,r}(x)\,(x\,T)\,W_0\left[B\left(1-\frac{x}{r}\right)^{\frac{1}{d}}\right]}{(1-c)\left[1\pm\varepsilon_{c,d,r}(x)\right](r-x)\left(1+W_0\left[B\left(1-\frac{x}{r}\right)^{\frac{1}{d}}\right]\right)}\mathrm{d}\boldsymbol{p}. \tag{40}$$

The differentiations of Eqs. (38), (39) and (40) with respect to μ give

$$\frac{\partial n}{\partial\mu}=\frac{\pm g}{2\pi^2 T}\int_0^\infty \frac{\boldsymbol{p}^2\,\varepsilon_{c,d,r}(x)\,W_0\left[B\left(1-\frac{x}{r}\right)^{\frac{1}{d}}\right]^2}{(d-d\,c)\left[1\pm\varepsilon_{c,d,r}(x)\right]r^2\,(1-x/r)^2\left(1+W_0\left[B\left(1-\frac{x}{r}\right)^{\frac{1}{d}}\right]\right)^3}\mathrm{d}\boldsymbol{p}$$

$$\mp\frac{g}{2\pi^2 T}\int_0^\infty \frac{\boldsymbol{p}^2\,\varepsilon_{c,d,r}(x)\,W_0\left[B\left(1-\dfrac{x}{r}\right)^{\frac{1}{d}}\right]}{(d-d\,c)\,[1\pm\varepsilon_{c,d,r}(x)]\,r^2\,(1-x/r)^2\left(1+W_0\left[B\left(1-\dfrac{x}{r}\right)^{\frac{1}{d}}\right]\right)^2}\mathrm{d}\boldsymbol{p}$$

$$-\frac{g}{2\pi^2 T}\int_0^\infty \frac{\boldsymbol{p}^2\,\zeta_{c,d,r}(x)\,W_0\left[B\left(1-\dfrac{x}{r}\right)^{\frac{1}{d}}\right]^2}{(1-c)^2\,[1\pm\varepsilon_{c,d,r}(x)]^2\,r^2\,(1-x/r)^2\left(1+W_0\left[B\left(1-\dfrac{x}{r}\right)^{\frac{1}{d}}\right]\right)^2}\mathrm{d}\boldsymbol{p}$$

$$\pm\frac{g}{2\pi^2 T}\int_0^\infty \frac{\boldsymbol{p}^2\,\varepsilon_{c,d,r}(x)\,W_0\left[B\left(1-\dfrac{x}{r}\right)^{\frac{1}{d}}\right]^2}{(1-c)^2\,[1\pm\varepsilon_{c,d,r}(x)]\,r^2\,(1-x/r)^2\left(1+W_0\left[B\left(1-\dfrac{x}{r}\right)^{\frac{1}{d}}\right]\right)^2}\mathrm{d}\boldsymbol{p}$$

$$\pm\frac{g}{2\pi^2 T}\int_0^\infty \frac{\boldsymbol{p}^2\,\varepsilon_{c,d,r}(x)\,W_0\left[B\left(1-\dfrac{x}{r}\right)^{\frac{1}{d}}\right]}{(1-c)\,[1\pm\varepsilon_{c,d,r}(x)]\,r^2\,(1-x/r)^2\left(1+W_0\left[B\left(1-\dfrac{x}{r}\right)^{\frac{1}{d}}\right]\right)}\mathrm{d}\boldsymbol{p}, \tag{41}$$

where

$$\zeta_{c,d,r}(x)=\exp\left[\frac{-2d}{1-c}\left(W_k\left[B\left(1-\frac{x}{r}\right)^{\frac{1}{d}}\right]-W_k[B]\right)\right]. \tag{42}$$

$$\frac{\partial\epsilon}{\partial\mu}=\frac{\pm g\,\mu}{2\pi^2 T}\int_0^\infty \frac{\boldsymbol{p}^2\,\varepsilon_{c,d,r}(x)\,\left(W_0\left[B\left(1-\dfrac{x}{r}\right)^{\frac{1}{d}}\right]\right)^2}{(d-d\,c)\,[1\pm\varepsilon_{c,d,r}(x)]\,r^2\,(1-x/r)^2\left(1+W_0\left[B\left(1-\dfrac{x}{r}\right)^{\frac{1}{d}}\right]\right)^3}\mathrm{d}\boldsymbol{p}$$

$$\mp\frac{g\,\mu}{2\pi^2 T}\int_0^\infty \frac{\boldsymbol{p}^2\,\varepsilon_{c,d,r}(x)\,W_0\left[B\left(1-\dfrac{x}{r}\right)^{\frac{1}{d}}\right]}{(d-d\,c)\,[1\pm\varepsilon_{c,d,r}(x)]\,r^2\,(1-x/r)^2\left(1+W_0\left[B\left(1-\dfrac{x}{r}\right)^{\frac{1}{d}}\right]\right)^2}\mathrm{d}\boldsymbol{p}$$

$$-\frac{g\,\mu}{2\pi^2 T}\int_0^\infty \frac{\boldsymbol{p}^2\,\zeta_{c,d,r}(x)\,W_0\left[B\left(1-\dfrac{x}{r}\right)^{\frac{1}{d}}\right]^2}{(1-c)^2\,[1\pm\varepsilon_{c,d,r}(x)]\,r^2\,(1-x/r)^2\left(1+W_0\left[B\left(1-\dfrac{x}{r}\right)^{\frac{1}{d}}\right]\right)^2}\mathrm{d}\boldsymbol{p}$$

$$\pm\frac{g\,\mu}{2\pi^2 T}\int_0^\infty \frac{\boldsymbol{p}^2\,\varepsilon_{c,d,r}(x)\,W_0\left[B\left(1-\dfrac{x}{r}\right)^{\frac{1}{d}}\right]^2}{(1-c)^2\,[1\pm\varepsilon_{c,d,r}(x)]\,r^2\,(1-x/r)^2\left(1+W_0\left[B\left(1-\dfrac{x}{r}\right)^{\frac{1}{d}}\right]\right)^2}\mathrm{d}\boldsymbol{p}$$

$$\pm\frac{g\,\mu}{2\pi^2 T}\int_0^\infty \frac{\boldsymbol{p}^2\,\varepsilon_{c,d,r}(x)\,W_0\left[B\left(1-\dfrac{x}{r}\right)^{\frac{1}{d}}\right]}{(1-c)\,[1\pm\varepsilon_{c,d,r}(x)]\,r^2\,(1-x/r)^2\left(1+W_0\left[B\left(1-\dfrac{x}{r}\right)^{\frac{1}{d}}\right]\right)}\mathrm{d}\boldsymbol{p}$$

$$\mp\frac{g}{2\pi^2 T}\int_0^\infty \frac{\boldsymbol{p}^2\,\varepsilon_{c,d,r}(x)\,(x\,T)\,W_0\left[B\left(1-\dfrac{x}{r}\right)^{\frac{1}{d}}\right]^2}{(d-d\,c)\,[1\pm\varepsilon_{c,d,r}(x)]\,r^2\,(1-x/r)^2\left(1+W_0\left[B\left(1-\dfrac{x}{r}\right)^{\frac{1}{d}}\right]\right)^3}\mathrm{d}\boldsymbol{p}$$

$$\pm\frac{g}{2\pi^2 T}\int_0^\infty \frac{\boldsymbol{p}^2\,\varepsilon_{c,d,r}(x)\,(x\,T)\,W_0\left[B\left(1-\frac{x}{r}\right)^{\frac{1}{d}}\right]}{(d-d\,c)\,[1\pm\varepsilon_{c,d,r}(x)]\,r^2\,(1-x/r)^2\left(1+W_0\left[B\left(1-\frac{x}{r}\right)^{\frac{1}{d}}\right]\right)^2}\mathrm{d}\boldsymbol{p}$$

$$+\frac{g}{2\pi^2 T}\int_0^\infty \frac{\boldsymbol{p}^2\,\zeta_{c,d,r}(x)\,(x\,T)\,W_0\left[B\left(1-\frac{x}{r}\right)^{\frac{1}{d}}\right]^2}{(1-c)^2\,[1\pm\varepsilon_{c,d,r}(x)]\,r^2\,(1-x/r)^2\left(1+W_0\left[B\left(1-\frac{x}{r}\right)^{\frac{1}{d}}\right]\right)^2}\mathrm{d}\boldsymbol{p}$$

$$\mp\frac{g}{2\pi^2 T}\int_0^\infty \frac{\boldsymbol{p}^2\,\varepsilon_{c,d,r}(x)\,(x\,T)\,W_0\left[B\left(1-\frac{x}{r}\right)^{\frac{1}{d}}\right]^2}{(1-c)^2\,[1\pm\varepsilon_{c,d,r}(x)]\,r^2\,(1-x/r)^2\left(1+W_0\left[B\left(1-\frac{x}{r}\right)^{\frac{1}{d}}\right]\right)^2}\mathrm{d}\boldsymbol{p}$$

$$\mp\frac{g}{2\pi^2 T}\int_0^\infty \frac{\boldsymbol{p}^2\,\varepsilon_{c,d,r}(x)\,(x\,T)\,W_0\left[B\left(1-\frac{x}{r}\right)^{\frac{1}{d}}\right]}{(1-c)\,[1\pm\varepsilon_{c,d,r}(x)]\,r^2\,(1-x/r)^2\left(1+W_0\left[B\left(1-\frac{x}{r}\right)^{\frac{1}{d}}\right]\right)}\mathrm{d}\boldsymbol{p}, \quad (43)$$

$$\frac{\partial s}{\partial \mu}=\frac{\mp g}{2\pi^2 T^2}\int_0^\infty \frac{\boldsymbol{p}^2\,\varepsilon_{c,d,r}(x)\,(x\,T)\,W_0\left[B\left(1-\frac{x}{r}\right)^{\frac{1}{d}}\right]^2}{(d-d\,c)\,[1\pm\varepsilon_{c,d,r}(x)]\,r^2\,(1-x/r)^2\left(1+W_0\left[B\left(1-\frac{x}{r}\right)^{\frac{1}{d}}\right]\right)^3}\mathrm{d}\boldsymbol{p}$$

$$\pm\frac{g}{2\pi^2 T^2}\int_0^\infty \frac{\boldsymbol{p}^2\,\varepsilon_{c,d,r}(x)\,(x\,T)\,W_0\left[B\left(1-\frac{x}{r}\right)^{\frac{1}{d}}\right]}{(d-d\,c)\,[1\pm\varepsilon_{c,d,r}(x)]\,r^2\,(1-x/r)^2\left(1+W_0\left[B\left(1-\frac{x}{r}\right)^{\frac{1}{d}}\right]\right)^2}\mathrm{d}\boldsymbol{p}$$

$$+\frac{g}{2\pi^2 T^2}\int_0^\infty \frac{\boldsymbol{p}^2\,\zeta_{c,d,r}(x)\,(x\,T)\,W_0\left[B\left(1-\frac{x}{r}\right)^{\frac{1}{d}}\right]^2}{(1-c)^2\,[1\pm\varepsilon_{c,d,r}(x)]^2\,r^2\,(1-x/r)^2\left(1+W_0\left[B\left(1-\frac{x}{r}\right)^{\frac{1}{d}}\right]\right)^2}\mathrm{d}\boldsymbol{p}$$

$$\mp\frac{g}{2\pi^2 T^2}\int_0^\infty \frac{\boldsymbol{p}^2\,\varepsilon_{c,d,r}(x)\,(x\,T)\,W_0\left[B\left(1-\frac{x}{r}\right)^{\frac{1}{d}}\right]^2}{(1-c)^2\,[1\pm\varepsilon_{c,d,r}(x)]\,r^2\,(1-x/r)^2\left(1+W_0\left[B\left(1-\frac{x}{r}\right)^{\frac{1}{d}}\right]\right)^2}\mathrm{d}\boldsymbol{p}$$

$$\mp\frac{g}{2\pi^2 T^2}\int_0^\infty \frac{\boldsymbol{p}^2\,\varepsilon_{c,d,r}(x)\,(x\,T)\,W_0\left[B\left(1-\frac{x}{r}\right)^{\frac{1}{d}}\right]}{(1-c)\,[1\pm\varepsilon_{c,d,r}(x)]\,r^2\,(1-x/r)^2\left(1+W_0\left[B\left(1-\frac{x}{r}\right)^{\frac{1}{d}}\right]\right)}\mathrm{d}\boldsymbol{p}, \quad (44)$$

From the substitution from Eqs. (41), (43), (44) and (55) into Eq. (21), we get

$$\left.\frac{\partial p}{\partial \mu}\right|_T = n. \quad (45)$$

Also, from Eqs. (39) and (40), we get a direct relation between entropy and energy density,

$$s=\frac{p}{T}+\frac{\epsilon}{T}-\frac{\mu\,n}{T}. \quad (46)$$

Thus, at constant n and p the differentiation of entropy density with respect to energy density leads to

$$\frac{\partial s}{\partial \epsilon}=\frac{1}{T}, \quad (47)$$

which proves the thermodynamic consistency, Eq. (12).

Also, from Eq. (46) we can write another form of energy density

$$\epsilon = T\,s - p + \mu\,n. \quad (48)$$

By differentiating the energy density with respect to n, we get

$$\left.\frac{\partial \epsilon}{\partial n}\right|_s = -\frac{\partial p}{\partial n}+\mu+n\frac{\partial \mu}{\partial n} = -\frac{\partial p}{\partial \mu}\frac{\partial \mu}{\partial n}+\mu+n\frac{\partial \mu}{\partial n}. \quad (49)$$

Then, by substituting from Eq. (45) into the previous equation,

$$\left.\frac{\partial\epsilon}{\partial n}\right|_s = \mu, \tag{50}$$

which is a proof of the thermodynamic self-consistency.

To prove the fourth equation in Eq. (12), the differentiations of Eqs. (38), (39) and (40) with respect to T read

$$\begin{aligned}
\frac{\partial n}{\partial T} = & \frac{-g}{2\pi^2 T^2}\int_0^\infty \frac{\boldsymbol{p}^2\,\varepsilon_{c,d,r}(x)\,(x\,T)\,W_0\left[B\left(1-\frac{x}{r}\right)^{\frac{1}{d}}\right]^2}{(d-d\,c)\left[1\pm\varepsilon_{c,d,r}(x)\right]r^2\,(1-x/r)^2\left(1+W_0\left[B\left(1-\frac{x}{r}\right)^{\frac{1}{d}}\right]\right)^3}\mathrm{d}\boldsymbol{p} \\
& \pm\frac{g}{2\pi^2 T^2}\int_0^\infty \frac{\boldsymbol{p}^2\,\varepsilon_{c,d,r}(x)\,(x\,T)\,W_0\left[B\left(1-\frac{x}{r}\right)^{\frac{1}{d}}\right]}{(d-d\,c)\left[1\pm\varepsilon_{c,d,r}(x)\right]r^2\,(1-x/r)^2\left(1+W_0\left[B\left(1-\frac{x}{r}\right)^{\frac{1}{d}}\right]\right)^2}\mathrm{d}\boldsymbol{p} \\
& +\frac{g}{2\pi^2 T^2}\int_0^\infty \frac{\boldsymbol{p}^2\,\zeta_{c,d,r}(x)\,(x\,T)\,W_0\left[B\left(1-\frac{x}{r}\right)^{\frac{1}{d}}\right]^2}{(1-c)^2\left[1\pm\varepsilon_{c,d,r}(x)\right]^2 r^2\,(1-x/r)^2\left(1+W_0\left[B\left(1-\frac{x}{r}\right)^{\frac{1}{d}}\right]\right)^2}\mathrm{d}\boldsymbol{p} \\
& \mp\frac{g}{2\pi^2 T^2}\int_0^\infty \frac{\boldsymbol{p}^2\,\varepsilon_{c,d,r}(x)\,(x\,T)\,W_0\left[B\left(1-\frac{x}{r}\right)^{\frac{1}{d}}\right]^2}{(1-c)^2\left[1\pm\varepsilon_{c,d,r}(x)\right]r^2\,(1-x/r)^2\left(1+W_0\left[B\left(1-\frac{x}{r}\right)^{\frac{1}{d}}\right]\right)^2}\mathrm{d}\boldsymbol{p} \\
& \mp\frac{g}{2\pi^2 T^2}\int_0^\infty \frac{\boldsymbol{p}^2\,\varepsilon_{c,d,r}(x)\,(x\,T)\,W_0\left[B\left(1-\frac{x}{r}\right)^{\frac{1}{d}}\right]}{(1-c)\left[1\pm\varepsilon_{c,d,r}(x)\right]r^2\,(1-x/r)^2\left(1+W_0\left[B\left(1-\frac{x}{r}\right)^{\frac{1}{d}}\right]\right)}\mathrm{d}\boldsymbol{p},
\end{aligned} \tag{51}$$

$$\begin{aligned}
\frac{\partial \epsilon}{\partial T} = & \frac{\pm g}{2\pi^2 T^2}\int_0^\infty \frac{\boldsymbol{p}^2\,\varepsilon_{c,d,r}(x)\,(x\,T)^2\,W_0\left[B\left(1-\frac{x}{r}\right)^{\frac{1}{d}}\right]^2}{(d-d\,c)\left[1\pm\varepsilon_{c,d,r}(x)\right]r^2\,(1-x/r)^2\left(1+W_0\left[B\left(1-\frac{x}{r}\right)^{\frac{1}{d}}\right]\right)^3}\mathrm{d}\boldsymbol{p} \\
& \mp\frac{g}{2\pi^2 T^2}\int_0^\infty \frac{\boldsymbol{p}^2\,\varepsilon_{c,d,r}(x)\,(x\,T)^2\,W_0\left[B\left(1-\frac{x}{r}\right)^{\frac{1}{d}}\right]}{(d-d\,c)\left[1\pm\varepsilon_{c,d,r}(x)\right]r^2\,(1-x/r)^2\left(1+W_0\left[B\left(1-\frac{x}{r}\right)^{\frac{1}{d}}\right]\right)^2}\mathrm{d}\boldsymbol{p} \\
& -\frac{g}{2\pi^2 T}\int_0^\infty \frac{\boldsymbol{p}^2\,\zeta_{c,d,r}(x)\,(x\,T)^2\,W_0\left[B\left(1-\frac{x}{r}\right)^{\frac{1}{d}}\right]^2}{(1-c)^2\left[1\pm\varepsilon_{c,d,r}(x)\right]r^2\,(1-x/r)^2\left(1+W_0\left[B\left(1-\frac{x}{r}\right)^{\frac{1}{d}}\right]\right)^2}\mathrm{d}\boldsymbol{p} \\
& \pm\frac{g}{2\pi^2 T^2}\int_0^\infty \frac{\boldsymbol{p}^2\,\varepsilon_{c,d,r}(x)\,(x\,T)^2\,W_0\left[B\left(1-\frac{x}{r}\right)^{\frac{1}{d}}\right]^2}{(1-c)^2\left[1\pm\varepsilon_{c,d,r}(x)\right]r^2\,(1-x/r)^2\left(1+W_0\left[B\left(1-\frac{x}{r}\right)^{\frac{1}{d}}\right]\right)^2}\mathrm{d}\boldsymbol{p} \\
& \pm\frac{g}{2\pi^2 T^2}\int_0^\infty \frac{\boldsymbol{p}^2\,\varepsilon_{c,d,r}(x)\,(x\,T)^2\,W_0\left[B\left(1-\frac{x}{r}\right)^{\frac{1}{d}}\right]}{(1-c)\left[1\pm\varepsilon_{c,d,r}(x)\right]r^2\,(1-x/r)^2\left(1+W_0\left[B\left(1-\frac{x}{r}\right)^{\frac{1}{d}}\right]\right)}\mathrm{d}\boldsymbol{p}
\end{aligned}$$

$$\mp\frac{g\,\mu}{2\pi^2T^2}\int_0^\infty \frac{\boldsymbol{p}^2\,\varepsilon_{c,d,r}(x)\,(x\,T)\,\left(W_0\left[B\left(1-\frac{x}{r}\right)^{\frac{1}{d}}\right]\right)^2}{(d-d\,c)\,[1\pm\varepsilon_{c,d,r}(x)]\,r^2\,(1-x/r)^2\left(1+W_0\left[B\left(1-\frac{x}{r}\right)^{\frac{1}{d}}\right]\right)^3}\mathrm{d}\boldsymbol{p}$$

$$\pm\frac{g\,\mu}{2\pi^2T^2}\int_0^\infty \frac{\boldsymbol{p}^2\,\varepsilon_{c,d,r}(x)\,(x\,T)\,W_0\left[B\left(1-\frac{x}{r}\right)^{\frac{1}{d}}\right]}{(d-d\,c)\,[1\pm\varepsilon_{c,d,r}(x)]\,r^2\,(1-x/r)^2\left(1+W_0\left[B\left(1-\frac{x}{r}\right)^{\frac{1}{d}}\right]\right)^2}\mathrm{d}\boldsymbol{p}$$

$$+\frac{g\,\mu}{2\pi^2T^2}\int_0^\infty \frac{\boldsymbol{p}^2\,\zeta_{c,d,r}(x)\,(x\,T)\,W_0\left[B\left(1-\frac{x}{r}\right)^{\frac{1}{d}}\right]^2}{(1-c)^2\,[1\pm\varepsilon_{c,d,r}(x)]\,r^2\,(1-x/r)^2\left(1+W_0\left[B\left(1-\frac{x}{r}\right)^{\frac{1}{d}}\right]\right)^2}\mathrm{d}\boldsymbol{p}$$

$$\mp\frac{g\,\mu}{2\pi^2T^2}\int_0^\infty \frac{\boldsymbol{p}^2\,\varepsilon_{c,d,r}(x)\,(x\,T)\,W_0\left[B\left(1-\frac{x}{r}\right)^{\frac{1}{d}}\right]^2}{(1-c)^2\,[1\pm\varepsilon_{c,d,r}(x)]\,r^2\,(1-x/r)^2\left(1+W_0\left[B\left(1-\frac{x}{r}\right)^{\frac{1}{d}}\right]\right)^2}\mathrm{d}\boldsymbol{p}$$

$$\mp\frac{g\,\mu}{2\pi^2T^2}\int_0^\infty \frac{\boldsymbol{p}^2\,\varepsilon_{c,d,r}(x)\,(x\,T)\,W_0\left[B\left(1-\frac{x}{r}\right)^{\frac{1}{d}}\right]}{(1-c)\,[1\pm\varepsilon_{c,d,r}(x)]\,r^2\,(1-x/r)^2\left(1+W_0\left[B\left(1-\frac{x}{r}\right)^{\frac{1}{d}}\right]\right)}\mathrm{d}\boldsymbol{p}, \tag{52}$$

$$\frac{\partial s}{\partial T}=\frac{\pm g}{2\pi^2T^3}\int_0^\infty \frac{\boldsymbol{p}^2\,\varepsilon_{c,d,r}(x)\,(x\,T)^2\,W_0\left[B\left(1-\frac{x}{r}\right)^{\frac{1}{d}}\right]^2}{(d-d\,c)\,[1\pm\varepsilon_{c,d,r}(x)]\,r^2\,(1-x/r)^2\left(1+W_0\left[B\left(1-\frac{x}{r}\right)^{\frac{1}{d}}\right]\right)^3}\mathrm{d}\boldsymbol{p}$$

$$\mp\frac{g}{2\pi^2T^3}\int_0^\infty \frac{\boldsymbol{p}^2\,\varepsilon_{c,d,r}(x)\,(x\,T)^2\,W_0\left[B\left(1-\frac{x}{r}\right)^{\frac{1}{d}}\right]}{(d-d\,c)\,[1\pm\varepsilon_{c,d,r}(x)]\,r^2\,(1-x/r)^2\left(1+W_0\left[B\left(1-\frac{x}{r}\right)^{\frac{1}{d}}\right]\right)^2}\mathrm{d}\boldsymbol{p}$$

$$-\frac{g}{2\pi^2T^3}\int_0^\infty \frac{\boldsymbol{p}^2\,\zeta_{c,d,r}(x)\,(x\,T)^2\,W_0\left[B\left(1-\frac{x}{r}\right)^{\frac{1}{d}}\right]^2}{(1-c)^2\,[1\pm\varepsilon_{c,d,r}(x)]^2\,r^2\,(1-x/r)^2\left(1+W_0\left[B\left(1-\frac{x}{r}\right)^{\frac{1}{d}}\right]\right)^2}\mathrm{d}\boldsymbol{p}$$

$$\pm\frac{g}{2\pi^2T^3}\int_0^\infty \frac{\boldsymbol{p}^2\,\varepsilon_{c,d,r}(x)\,(x\,T)^2\,W_0\left[B\left(1-\frac{x}{r}\right)^{\frac{1}{d}}\right]^2}{(1-c)^2\,[1\pm\varepsilon_{c,d,r}(x)]\,r^2\,(1-x/r)^2\left(1+W_0\left[B\left(1-\frac{x}{r}\right)^{\frac{1}{d}}\right]\right)^2}\mathrm{d}\boldsymbol{p}$$

$$\pm\frac{g}{2\pi^2T^3}\int_0^\infty \frac{\boldsymbol{p}^2\,\varepsilon_{c,d,r}(x)\,(x\,T)^2\,W_0\left[B\left(1-\frac{x}{r}\right)^{\frac{1}{d}}\right]}{(1-c)\,[1\pm\varepsilon_{c,d,r}(x)]\,r^2\,(1-x/r)^2\left(1+W_0\left[B\left(1-\frac{x}{r}\right)^{\frac{1}{d}}\right]\right)}\mathrm{d}\boldsymbol{p}. \tag{53}$$

Then, the substitution from Eqs. (40), (51), (52) and (53) into Eq. (29) gives

$$\left.\frac{\partial p}{\partial T}\right|_{\mu}=s. \tag{54}$$

So far, we have proved that the definitions of temperature, number density, chemical potential and entropy density within our formalism for nonextensive quantum statistics lead to expressions which satisfy the first law of thermodynamics.

4 Confronting our calculations with various experimental results

The statistical-thermal models have been successful in reproducing particle ratios and yields at different energies [1, 8–10, 35–37]. In these models, the hadronic phase can be modelled at chemical and thermal equilibrium. Accordingly, fitting parameters can then be identified. They construct a set of various thermal parameters. The most significant ones are the chemical freeze-out temperature and baryon chemical potential [1].

The deconfined phase is dominated by quarks and gluons degrees-of-freedom. Most of their information cannot be recognized due to the nature of such partonic QCD matter. While the integrated particle-yields are successfully constructed in the final state, the transverse momentum distribution should be described by a combination of transverse flow and statistical distributions (particle ratios and yields). In other words, the latter contains contributions from earlier stages of the collision, while the particle ratios and yields are conjectured to be fixed during the chemical and thermal equilibrium stages. Thus, we plan to confront this new generic approach with both types of experimental results, namely, transverse momentum spectra, and particle ratios and yields. This shall be introduced in the sections that follow. We intend to prove whether the proposed approach is indeed able to reflect the statistical nature of the system of interest.

4.1 Transverse momentum distributions

The particle distributions at large transverse momenta are indeed very interesting phenomena in high-energy particle production, but as discussed by Bialas [16], the applicability of the statistical-thermal models in this regime of the transverse momenta is debatable. These models, either extensive or nonextensive, are excellent approaches at low p_T. The scope of this paper is the examination of the thermodynamic self-consistency and then implementing the proposed approach in characterizing both transverse momentum distributions and particle ratios and yields.

As discussed in the introduction, the hadronic clusters are assumed to undergo thermal decays, but simultaneously move in the transverse direction with a fluctuation Lotentz factor [16]. Recently, this statistical cluster-decay model was implemented in high-energy physics [17] and it was concluded that the well-known Tsallis distribution can be obtained in a very special case, namely, the fluctuations of the Lorentz factor and the relativistic temperature are given by Beta and Gamma distributions, respectively. The role of the statistical cluster-decay and its possible connections with the approach proposed in the present work shall be subjects of future works.

We first implement the generic nonextensive statistical approach [27] in order to reproduce various transverse momentum distributions measured in different experiments [23, 38–42]. For quantum statistics, the total number of particles can be determined from Eq. (55)

$$N=\pm\frac{V}{8\pi^3}\sum_i g_i\int_0^\infty \frac{\boldsymbol{p}^2\,\varepsilon_{c,d,r}(x_i)\,W_0\left[B\left(1-\frac{x_i}{r}\right)^{\frac{1}{d}}\right]}{(1-c)\left[1\pm\varepsilon_{c,d,r}(x_i)\right](r-x_i)\left(1+W_0\left[B\left(1-\frac{x_i}{r}\right)^{\frac{1}{d}}\right]\right)}\mathrm{d}^3\boldsymbol{p}, \tag{55}$$

where $x_i=(\mu-E_i)/T$, $i\in[\pi^+,\mathtt{K}^+,\mathtt{p}]$, and $r=[1-c+cd]^{-1}$. Their degeneracy factors read $g_{\pi^+}=g_{\mathtt{K}^+}=g_{\mathtt{p}}=1$. For antiparticles, μ is replaced by $-\mu$.

The corresponding momentum distribution for particles (or antiparticles) is given as

$$\frac{1}{2\pi}\frac{E\mathrm{d}^3N}{\mathrm{d}^3p}=\pm\frac{V}{8\pi^3}\sum_i g_iE_iT\frac{\varepsilon_{c,d,r}(x_i)\;W_0\left[B\left(1-\frac{x_i}{r}\right)^{\frac{1}{d}}\right]}{(1-c)\left[1\pm\varepsilon_{c,d,r}(x_i)\right](rT-\mu+E_i)\left(1+W_0\left[B\left(1-\frac{x_i}{r}\right)^{\frac{1}{d}}\right]\right)}, \tag{56}$$

where $\varepsilon_{c,d,r}(x_i)$ is defined in Eq. (4). In terms of rapidity (y) and transverse mass ($m_{T\,i}=\sqrt{p_T^2+m_i^2}$), the transverse momentum distribution can be given as

$$\frac{1}{2\pi}\frac{\mathrm{d}^2N}{\mathrm{d}y m_T\mathrm{d}m_T}=\pm\frac{V}{8\pi^3}\sum_i g_iTm_{T\,i}\cosh y \tag{57}$$

$$\times\frac{\varepsilon_{c,d,r}\left(\frac{\mu-m_{T\,i}\cosh y}{T}\right)\,W_0\left[B\left(1-\frac{\mu-m_{T\,i}\cosh y}{rT}\right)^{\frac{1}{d}}\right]}{(1-c)\left[1\pm\varepsilon_{c,d,r}\left(\frac{\mu-m_{T\,i}\cosh y}{T}\right)\right](rT+m_{T\,i}\cosh y-\mu)\left(1+W_0\left[B\left(1-\frac{\mu-m_{T\,i}\cosh y}{rT}\right)^{\frac{1}{d}}\right]\right)}.$$

At mid-rapidity, i.e. $y=0$, and $\mu=0$,

$$\frac{1}{2\pi}\frac{\mathrm{d}^2N}{\mathrm{d}ym_T\mathrm{d}m_T}=\pm\frac{V}{8\pi^3}\sum_i g_iTm_{Ti} \times\frac{\varepsilon_{c,d,r}\left(\frac{-m_{Ti}}{T}\right)W_0\left[B\left(1-\frac{(-m_{Ti})}{rT}\right)^{\frac{1}{d}}\right]}{(1-c)\left[1\pm\varepsilon_{c,d,r}\left(\frac{-m_{Ti}}{T}\right)\right](rT+m_{Ti})\left(1+W_0\left[B\left(1-\frac{(-m_{Ti})}{rT}\right)^{\frac{1}{d}}\right]\right)}. \quad (58)$$

The transverse momentum distribution reads

$$\left.\frac{1}{2\pi}\frac{\mathrm{d}^2N}{p_\mathrm{T}\mathrm{d}y\mathrm{d}p_\mathrm{T}}\right|_{y=0}=\pm\frac{V}{8\pi^3}\sum_i g_iTm_{Ti} \times\frac{\varepsilon_{c,d,r}\left(\frac{-m_{Ti}}{T}\right)W_0\left[B\left(1-\frac{(-m_{Ti})}{rT}\right)^{\frac{1}{d}}\right]}{(1-c)\left[1\pm\varepsilon_{c,d,r}\left(\frac{-m_{Ti}}{T}\right)\right](rT+m_{Ti})\left(1+W_0\left[B\left(1-\frac{(-m_{Ti})}{rT}\right)^{\frac{1}{d}}\right]\right)}. \quad (59)$$

At mid-rapidity, i.e. $y=0$, but $\mu\neq 0$

$$\left.\frac{1}{2\pi}\frac{\mathrm{d}^2N}{p_\mathrm{T}\mathrm{d}y\mathrm{d}p_\mathrm{T}}\right|_{y=0}=\pm\frac{V}{8\pi^3}\sum_i g_iTm_{Ti} \times\frac{\varepsilon_{c,d,r}\left(\frac{\mu-m_{Ti}}{T}\right)W_0\left[B\left(1-\frac{(\mu-m_{Ti})}{rT}\right)^{\frac{1}{d}}\right]}{(1-c)\left[1\pm\varepsilon_{c,d,r}\left(\frac{\mu-m_{Ti}}{T}\right)\right](rT-\mu+m_{Ti})\left(1+W_0\left[B\left(1-\frac{(\mu-m_{Ti})}{rT}\right)^{\frac{1}{d}}\right]\right)}. \quad (60)$$

We can now fit various transverse momentum distributions measured in different experiments, i.e. different types of collisions and different collision energies, rapidity, centrality, etc. by using Eq. (59) and Eq. (60) at mid-rapidity. Expression (60) takes into consideration vanishing and finite baryon chemical potentials [1, 43].

Figure 1 depicts the transverse momentum distributions for the charged particles K^+,π^+ and p and their antiparticles measured in different types of collisions at various collision energies; p+p collisions at 0.54 [38], 0.9, 2.36 and 7 TeV [23], p+Pb collisions at 5.02 TeV [41], Pb+Pb collisions at 2.76 TeV [42], d+Au collisions and Au+Au collisions at 0.2 TeV [39, 40]. This set of measured particles combines the momentum spectra of six charged particles. Here, we zoom out the smallest p_T region. The entire p_T spectra are illustrated in Fig. 2. All these distributions are fitted to the generic nonextensive statistical approach, Eq. (59). The resulting fit parameters are given in Table 1. For a better comparison, the p+p, p+A and A+A results are separately depicted in Fig. 1(a), (b), and (c), respectively.

The entire p_T-range is presented in Fig. 2. It is worth highlighting that the statistical fit was performed over the complete range of p_T. Figure 1 is there to zoom out a smaller p_T-window. In the panel (a), we can compare between the pp transverse momentum distributions at different collision energies. There are obvious trends with increasing collision energy $\mathrm{d}^2N/\mathrm{d}y\mathrm{d}p_\mathrm{T}$. Furthermore, at a given collision energy, $\mathrm{d}^2N/\mathrm{d}y\mathrm{d}p_\mathrm{T}$ exponentially decreases rapidly with increasing p_T.

All measurements are performed at mid-rapidity and we assume a vanishing chemical potential. The quality of the statistical fit looks excellent, see Table 1. In p+p collisions at 0.546 TeV, we find that $c\simeq 1$, while $d\simeq 1.35$. Similar values are also obtained in p+A and A+A collisions, panels (b) and (c). These two values of the equivalence class $(c,d)=(1,d)$ are associated with asymptotically stable systems. At the resulting d, which is positive, asymptotically stable systems - in turn - are associated with stretched exponential distributions [45],

$$\lim_{c\rightarrow 1}\varepsilon_{d,r}(x)=\exp\left\{-dr\left[(1-x/r)^{1/d}-1\right]\right\}. \quad (61)$$

The entropy becomes a stretched exponential [44] leads to the special case

$$\varepsilon_{d,r}(x)=r^{1-d}\,d^{-d}\exp(dr)\,\Gamma(1+d,dr-\ln x)-r\,x. \quad (62)$$

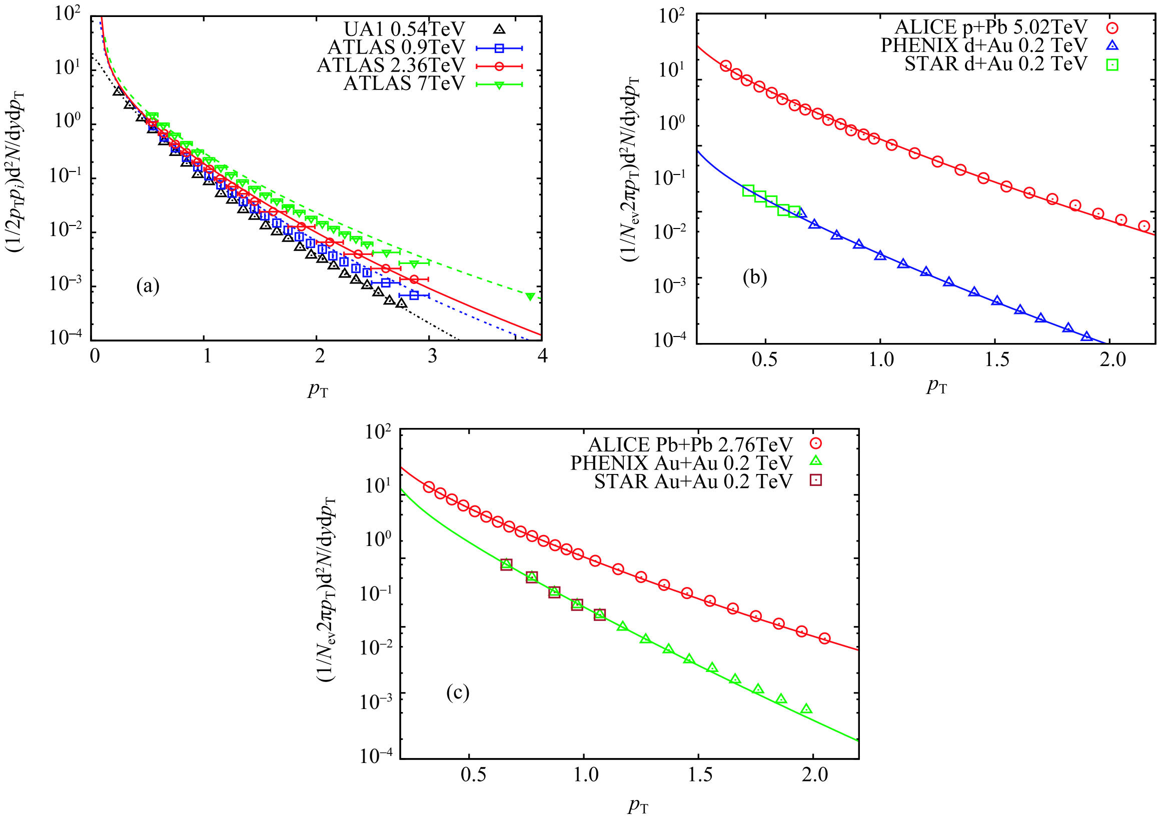

Fig. 1. (color online) Transverse momentum distributions for the charged particles K^+,π^+ and p and their antiparticles measured in the experiments UA1 [38], PHENIX [39], STAR [40], ATLAS [23] and ALICE [41, 42] (symbols) are compared with calculations from the generic nonextensive statistical approach (curves). The resulting fit parameters are listed in Table 1. The pp, pA and AA results are separately depicted in panels (a), (b) and (c), respectively.

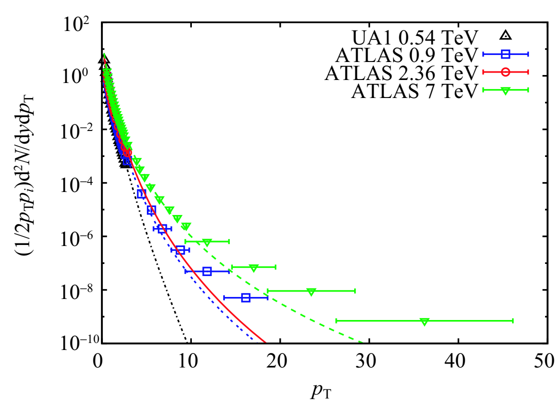

Fig. 2. (color online) The same as in Fig. 1 including the largest $p_{\rm T}$-region.

It has been proved that the numerical analysis becomes impossible without the general case of the Gamma-function, $\Gamma(a,b)=\int_b^{\infty}{\rm d}t\,t^{a-1}\exp(-t)$.

Furthermore, we observe that the ATLAS measurements are associated with positive c (close to unity), while d can be approximated as $d\simeq 1$. Such an equivalence class defines a nonextensive entropy which is linearly dependent on or - in other words - composed of extensive entropies, such as Renyi [46]. Its optimized entropy is given by probability distribution (p_i), which includes the Lambert function,

$$S_{\beta}=\sum_i p_i^{\beta}\ln\left(\frac{1}{p_i}\right), \qquad (63)$$

where $\beta\equiv c$ and p_i^{β} is the probability that the entire phase-space is occupied. Although this type of entropy looks analogous to the Tsallis one, $-\sum_i(1-p_i^q)/(1-q)$, it is apparently different, at least, as the latter reaches singularity, at $q=1$, the so-called Shannon limit. Further differences have been elaborated in Ref. [46].

It is worth highlighting that the resulting freezeout temperatures ($T_{\rm ch}$) rise with increasing collision energy ($\sqrt{s_{\rm NN}}$). Possible explanations of this observation are postponed for a future work. We focus on the discussion of their phenomenologies. The Tsallis nonextensive approach was also used in conducting the same study [47]. Accordingly, there is a remarkable difference between $T_{\rm ch}$ obtained from our approach and the one deduced from the Tsallis-type approach [47]. The latter are relatively smaller than the earlier results (compare Table 1 of the present work with Table 1 of Ref. [47]).

Figure 1(b) shows the transverse momentum distributions of the three charged particles K^+,π^+ and p and their antiparticles measured in d+Au collisions at 0.2 TeV and in p+Pb collisions at 5.02 TeV. The equivalence class can be constricted from $c \simeq 1$, and d. The latter is found to be almost energy-independent; 1.291 ± 0.006 at 0.2 TeV to 1.331 ± 0.004 at 5.02 TeV. The freezeout parameters are very interesting. The resulting freezeout temperature slightly increases from 170 ± 13.038 MeV at 0.2 TeV to 175 ± 13.228 MeV at 5.02 TeV, while the corresponding baryon chemical potential drops from 29 MeV at 0.2 TeV to 0 MeV at 5.02 TeV.

Figure 1(c) presents a comparison between A+A collisions at different collision energies; Au+Au collisions at 0.2 TeV and Pb+Pb collisions at 2.76 TeV for the momentum spectra of the three charged particles K^+,π^+ and p and their antiparticles. Despite the system size difference, we also find that $c \simeq 1$, while d slightly increases from 1.221 ± 0.055 at 0.2 TeV to 1.357 ± 0.023 at 2.76 TeV. The freezeout temperature shows an energy-independent behavior; 155 ± 12.450 MeV at 0.2 TeV to 165 ± 12.845 MeV at 2.76 TeV. The baryon chemical potential behaves similarly to in p+A collisions, shown in Fig. 1(b).

Table 1. Various parameters deduced for the statistical fit of the transverse momentum calculations based on the generic nonextensive statistical approach (present work) to various measurements, shown in Fig. 1.

experiment	$\sqrt{s_{NN}}$/TeV	centrality	T_{ch}/MeV	μ_b/MeV	d	c	χ^2
UA1 (p+p)	0.546	0%	110 ± 10.488	0.0	1.35 ± 0.135	0.999 ± 0.100	0.384
ATLAS (p+p)	0.9	0%	140 ± 11.832	0.0	1.03 ± 0.103	0.945 ± 0.095	0.766
ATLAS (p+p)	2.36	0%	160 ± 12.649	0.0	1.06 ± 0.106	0.945 ± 0.095	1.651
ATLAS (p+p)	7.0	0%	150 ± 12.247	0.0	1.05 ± 0.105	0.930 ± 0.093	1.115
PHENIX/STAR (d+Au)	0.2	0% − 20%	170 ± 13.038	29	1.291 ± 0.006	0.999 ± 0.001	1.884
ALICE (p+Pb)	5.02	0% − 5%	175 ± 13.228	0.0	1.333 ± 0.004	0.999 ± 0.001	0.902
PHENIX/STAR (Au+Au)	0.2	0% − 10%	155 ± 12.450	25	1.221 ± 0.055	0.999 ± 0.001	1.584
ALICE (Pb+Pb)	2.76	0% − 5%	165 ± 12.845	0.0	1.357 ± 0.023	0.999 ± 0.001	0.164

From the fit parameters listed in Table 1, we can summarize that except for the ATLAS measurements, $c \simeq 1$, while $d > 1$. These values are obtained for different system sizes and at various collision energies. They refer to nonextensivity but not of Tsallis type. We note again that the BG extensivity is guaranteed only at $c = d = 1$. It has been pointed out [16] that the Tsallis algebra, which is mainly implemented through replacing the exponential and logarithmic functions by their counterpart expressions in the Tsallis nonextensive approach, can be scaled as power laws. Such a scaling can also be obtained in the so-called statistical cluster-decay. Thus, the good fitting of the transverse momentum distributions by the Tsallis nonextensivity would be misleading [16], as the role of the statistical cluster-decay is apparently ignored. In a forthcoming work, we shall estimate the contribution of the statistical cluster-decay to the possible power-laws in the nonextensive fit, with a special emphasis on Tsallis-type nonextensivity.

In the section that follows, we confront our approach with different particle ratios and yields, which likely cannot be scaled as power laws, as such. The resulting (non)extensivity parameters are conjectured to shed light on the statistical nature of the particle production and whether it is an extensive or a nonextensive process, and if the latter, whether this follows Tsallis approach.

4.2 Particle ratios and yields

The particle ratios π^-/π^+, K^-/K^+, $\bar{p}/p$, $\bar{\Lambda}/\Lambda$, $\bar{\Omega}/\Omega$, $\bar{\Xi}/\Xi$, K^-/π^-, K^+/π^+, $\bar{p}/\pi^-$, p/π^+, Λ/π^-, Ω/π^-, and $\bar{\Xi}/\pi^+$ measured in Au+Au collisions in the STAR experiment at energies 200 GeV, 62.4 GeV, and 7.7 GeV are statistically fitted by means of the HRG model, in which the generic nonextensive statistical approach is implemented. The number density can be derived from the partition function and accordingly the particle ratios can be determined.

We take into account all possible decays into the particle of interest and their branching ratios. μ, T, c, and d are taken as free parameters. The strangeness chemical potential is calculated at each value assigned to μ, T, c, and d so that an overall strangeness conservation is guaranteed. The results depicted in Fig. 3 represent the best agreement between measurements and calculations, i.e. at the smallest χ^2 value. The results at 200 GeV [panel (a)], 62.4 GeV [panel (b)] and 7.7 GeV [panel (c)] are depicted in Fig. 3. We observe that the quality of the fits weakens with the collision energies; $\chi^2/\mathtt{dof} = 1.105$, $\chi^2/\mathtt{dof} = 2.771$ and $\chi^2/\mathtt{dof} = 8.146$ at 200 GeV, 62.4 GeV and 7.7 GeV, respectively.

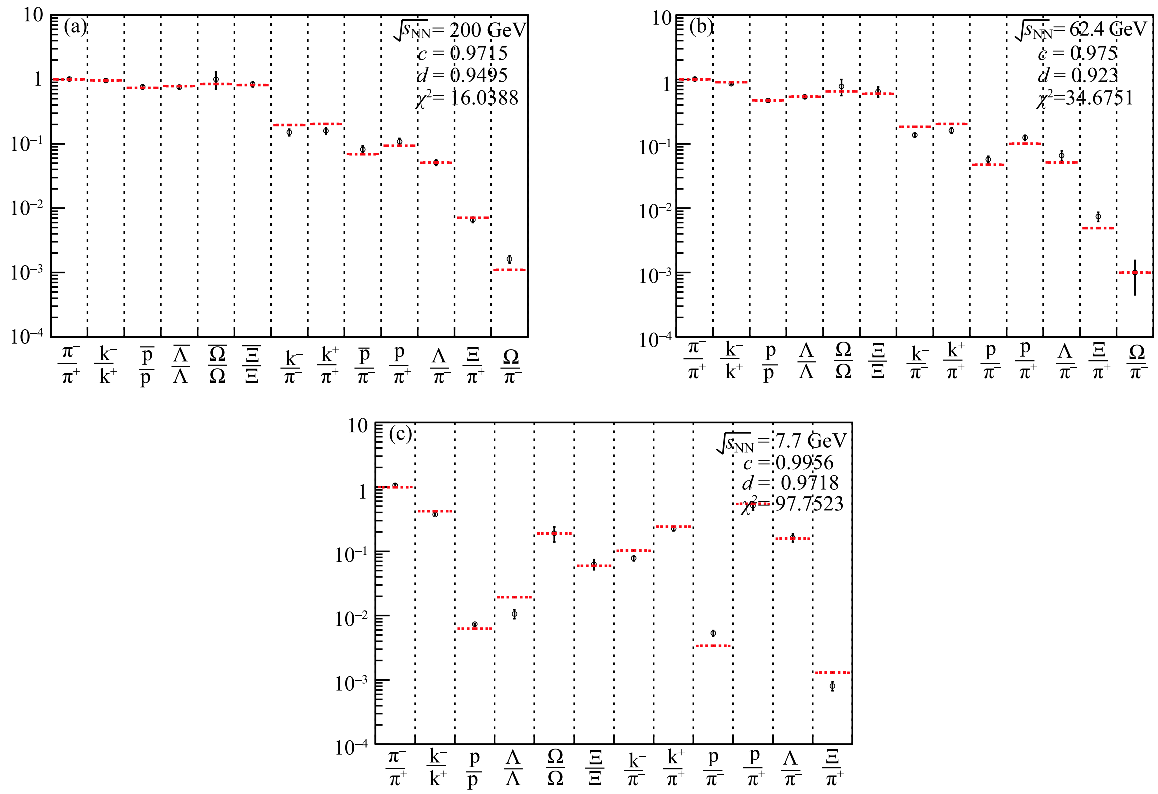

Fig. 3. Panel (a): different particle ratios deduced from the generic axiomatic-nonextensive statistical approach (dashed lines) are compared with the experimental results at 200 GeV (symbols). Panels (b) and (c) show the same but at 62.4 and 7.7 GeV, respectively. The exponents c, d and χ^2 are given in the top right corner.

As mentioned, our fits for the transverse momentum distributions and the debatable interpretation of whether the resulting parameters are due to power laws stemming from Tsallis-algebra should be a subject of a future work. Here, we have analysed another thermodynamic quantity, the particle ratios, which are conjectured to highlight the (non)extensivity, as they are not to be scaled as power laws. In light of this assumption, we can discuss the resulting parameters and their physical meanings.

The resulting freezeout temperature (T_{ch}) and baryon chemical potential (μ_{b}) can be summarized as follows.

- at 200 GeV, $T_{\text{ch}} = 148.05 \pm 12.168$ MeV and $\mu_{\text{b}} = 23.94 \pm 4.89$ MeV,
- at 62.4 GeV, $T_{\text{ch}} = 179.13 \pm 13.384$ MeV and $\mu_{\text{b}} = 57.33 \pm 7.57$ MeV, and
- at 7.7 GeV, $T_{\text{ch}} = 145.32 \pm 12.055$ MeV and $\mu_{\text{b}} = 384.3 \pm 19.6$ MeV,

which are obviously very compatible with those deduced from BG statistics [43]. The equivalence class reads

- At 200 GeV, $c = 0.971 \pm 0.097$ and $d = 0.949 \pm 0.09$,
- at 62.4 GeV, $c = 0.975 \pm 0.098$ and $d = 0.923 \pm 0.091$ and
- at 7.7 GeV, $c = 0.995 \pm 0.1$ and $d = 0.972 \pm 0.097$.

These can be approximated as both c and d lie below unity, referring neither to BG extensivity nor to Tsallis nonextensivity. This conclusion still needs further analysis at other collision energies. We shall devote a future work to examine such a relation.

In Fig. 4, we present fits for various particle yields, π^-, π^+, K^-, K^+, $\bar{p}$, p, $\bar{\Lambda}$, Λ, $\bar{\Omega}$, Ω, $\bar{\Xi}$, and Ξ, measured in Au+Au collisions in the STAR experiment (symbols) at 200 GeV, 62.4 GeV, and 7.7 GeV, respectively, fitted to calculations from the HRG model with generic nonextensive statistical approach (dashed lines). The equivalence class is given in the top-right corners of each graph. Together with the resulting freezeout parameters, they are listed in Table 2.

In summary, we have found that

- for p_{T} spectra except ATLAS, $c \simeq 1$ and $d > 1$. The nonextensive entropy is associated with stretched exponentials, where the Lambert function reaches its asymptotic stability.
- for ATLAS p_{T} spectra, $c < 1$, while $d \simeq 1$. The nonextensive entropy is linearly composed of extensive entropies. The reasons why the ATLAS measurements look different from the others shall be discussed in a future work.
- for particle ratios and yields, $c < 1$ and $d < 1$. This is known as (c, d)-entropy, where $d > 0$ and Lambert functions W_0 rise exponentially.

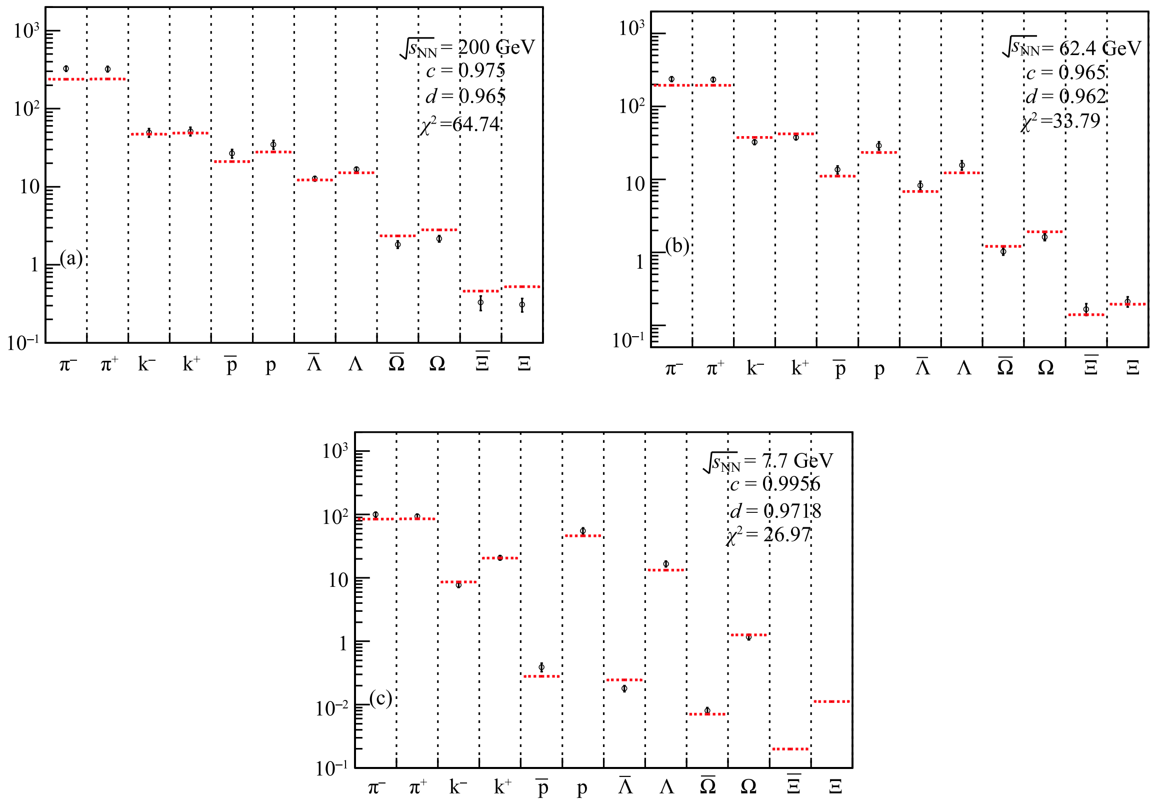

Fig. 4. (color online) The same as in Fig. 3 but for the particle yields.

Table 2. The freezeout parameters and equivalence class deduced for the statistical fit of the generic nonextensive statistical approach (present work) compared with the experimental results on particle yields, Fig. 4.

$\sqrt{s_{NN}}$/GeV	centrality	T_{ch}/MeV	μ_b/MeV	d	c	R/fm	χ^2
200	0%	160.54±12.67	25.20±5.02	0.965±0.097	0.975±0.098	2.044±1.126	5.395
62.4	0%	170.00±13.04	57.83±7.60	0.962±0.096	0.965±0.097	1.796±1.056	2.816
7.7	0%	147.31±12.14	388.08±19.7	0.972±0.097	0.995±0.101	1.848±1.071	2.701

5 Conclusions and outlook

We have presented a systematic study of the thermodynamic self-consistency of the generic axiomatic-nonextensive statistical approach, which is characterized by two asymptotic properties. To each of these, a scaling function was assigned. These scaling functions are estimated by exponents c and d for the first and second property, respectively, in the thermodynamic limit of grand-canonical ensembles of classical (Boltzmann) and quantum gas (Fermi-Dirac and Bose-Einstein) statistics of a gas composed of various hadron resonances. We started with the first and second laws of thermodynamics, which characterize the statistical system of interest. The thermodynamic properties of that system were determined and it was confirmed that both laws of thermodynamic are fully verified. We have proved that the definitions of temperature, number density, chemical potential and entropy density within the generic axiomatic-nonextensive classical and quantum statistical approach lead to expressions which satisfy the laws of thermodynamics.

The second part of this paper introduced implementations of the generic axiomatic-nonextensive statistical approach to high-energy physics. We started with the transverse momentum distributions measured in central collisions, in different system sizes and at various collision energies. We found that $c \simeq 1$ and $d > 1$, which describe nonextensive entropy associated with stretched exponentials, in which the Lambert function behaves asymptotically. For the ATLAS p_T spectra, $c < 1$, while $d \simeq 1$. This is nonextensive entropy, which linearly involves extensive entropies, such as Renyi. All these values differ from the equivalence class characterizing BG and Tsallis statistics. The role of statistical cluster decays was also highlighted. Their contributions to the possible power-laws should be first evaluated, so that those stemming from Tsallis-type nonextensivity can be determined.

We also calculated different particle ratios and yields, which likely are not to be scaled as power laws. From the resulting exponents c and d, we can judge whether the particle production is a (non)extensive process. We found that $c < 1$ and $d < 1$ referring to (c,d)-entropy, where the Lambert functions rise exponentially. This finding points to neither BG extensivity nor Tsallis nonextensivity.

From the statistical fit of both sets of experimental results [transverse momentum distribution (p_{T}) and particle ratios and yields], the resulting freezeout parameters, T_{ch} and μ_{b}, are fairly compatible with those deduced from BG statistics. We believe that the statistical properties, whether extensive or nonextensive, should not be related to intensive or extensive thermodynamic quantities, such as temperature and baryon chemical potential. These are strongly associated with the proposed equivalence class (c,d). The latter characterizes BG, or Tsallis or even generic statistics, where $(1,1)$, or $(c,0)$ or (c,d), respectively. The thermodynamic quantities are conjectured to partly manifest the physical properties of the system of interest, while the nature of (non)extensivity characterizes the statistical properties.

Finally, we conclude that the proposed generic nonextensive statistical approach is thermodynamically self-consistent and able to reveal the statistical nature of various processes taking place in high-energy collisions, such as transverse momentum spectra and particle ratios and yields.

Many authors endorse the assumption that Tsallis-type nonextensivity originates in fluctuations, correlations and inter-particle interactions. We briefly discussed all these in the introduction. Wilk et al. [48] proposed that the nonextensive parameter (q) is related to fluctuations in the inverse temperature. It is believed that the temperature reflects the impact of the nonextensivity. Since this interesting topic lies out of the scope of this paper, we plan in a future work to examine the possibilities that the equivalence class (c,d), instead of the temperature, might affect some or all of the physical processes, fluctuations, correlations and inter-particle interactions.

References

1 A. N. Tawfik, Int. J. Mod. Phys. A, **29**: 1430021 (2014)
2 A. Tawfik, J. Phys. G, **40**: 055109 (2013)
3 R. Hagedorn, Nuovo Cimento Suppl., **3**: 147 (1965)
4 A. Tawfik, Prog. Theor. Phys., **126**: 279 (2011)
5 C. Beck, Physica, A, **286**: 164 (2000)
6 I. Bediaga, E. M. F. Curado, and J. M. de Miranda, Physica A, **286**: 156 (2000)
7 W. M. Alberico, A. Lavagno, and P. Quarati, Eur. Phys. J. C, **12**: 499–506 (2000)
8 S. Tripathy et al., Eur. Phys. J. A, **52**: 289 (2016)
9 A. Khuntia et al, Eur. Phys. J. A, **52**: 292 (2016)
10 T. Bhattacharyya et al, Eur. Phys. J. A, **52**: 30 (2016)
11 A. Deppman, J. Phys. G, **41**: 055108 (2014)
12 W. M. Alberico et al, Physica A, **387**: 467 (2008)
13 T. Bhattacharyya, R. Sahoo, and P. Samantray, Eur. Phys. J. A, **52**: 283 (2016)
14 Q. A. Wong, Entropy, **5**: 220 (2003).
15 A. N. Tawfik, Eur. Phys. J. A, **52**: 253 (2016)
16 A. Bialas, Phys. Lett. B, **747**: 190 (2015)
17 G. Wilk and Z. Wlodarcyk, Phys. Lett. A, **379**: 2941 (2015)
18 C. Beck and E. G. D. Cohen, Physica A, **322**: 267 (2003)
19 F. Sattin, Eur. Phys. J. B, **49**: 219 (2006)
20 B. I. Abelev et al (STAR Collaboration), Phys. Rev. C, **75**: 064901 (2007)
21 A. Adare et al (PHENIX Collaboration), Phys. Rev. C, **83**: 052004 (2010)
22 K. Aamodt et al (ALICE Collaboration), Eur. Phys. J. C, **71**: 1655 (2011).
23 G. Aad et al (ATLAS Collaboration), New J. Phys., **13**: 053033 (2011)
24 V. Khachatryan et al (CMS Collaboration), JHEP, **05**: 064 (2011)
25 R. Hanel and S. Thurner, Europhys. Lett., **93**: 20006 (2011)
26 R. Hanel and S. Thurner, Europhys. Lett., **96**: 50003 (2011)
27 A. N. Tawfik, *Lattice QCD thermodynamics and RHIC-BES particle production within generic nonextensive statistics*, submitted to EPJA
28 A. S. Parvan, Eur. Phys. J. A, **51**: 108 (2015)
29 A. Deppman, Physica A, **391**: 6380 (2012)
30 A. S. Parvan, Phys. Lett. A, **350**: 331 (2006)
31 A. S. Parvan, Phys. Lett. A, **360**: 26 (2006)
32 J. Cleymans and D. Worku, J. Phys. G, **39**: 025006 (2012)
33 J. Letessier and J. Rafelski, *Hadrons and Quark-Gluon Plasma*, (Cambridge University Press, UK, 2004), p. 210
34 S. Thurner and R. Hanel, Int. J. Mod. Phys.: Conf. series, **16**: 105 (2012)
35 J. Cleymans, H. Oeschler, K. Redlich, and S. Wheaton, Phys. Rev. C, **73**: 034905 (2006)
36 A. Andronic, P. Braun-Munzinger, and J. Stachel, Nucl. Phys. A, **772**: 167 (2006)
37 F. Becattini, J. Manninen, and M. Gazdzicki, Phys. Rev. C, **73**: 044905 (2006)
38 C. Albajar et al (UA1 Collaboration), Nucl. Phys. B, **335**, 261 (1990)
39 A. Adare et al (PHENIX Collaboration), Phys. Rev. C, **88**: 024906 (2013)
40 B. I. Abelev et al (STAR Collaboration), Phys. Rev. C, **79**: 034909 (2009)
41 B. Abelev et al (ALICE Collaboration), Phys. Lett. B, **728**: 25 (2014)
42 B. Abelev et al (ALICE Collaboration), Phys. Rev. Lett. **109**: 252301 (2012)
43 A. N. Tawfik and E. Abbas, Phys. Part. Nucl. Lett., **12**: 521 (2015)
44 C. Anteneodo and A. R. Plastino, J. Phys A: Math. Gen., **32**: 1089 (1999)
45 R. Hanel and S. Thurner, arXir: 1005.0138 [physics.class-ph]
46 Fariel Shafee, IMA J. Appl. Math., **72**: 785 (2007)
47 J. Cleymans et al,Phys. Lett. B, **723**: 351 (2013)
48 G. Wilk and Z. Wlodarczyk, Phys. Rev. Lett., **84**: 2770 (2000)